Available online at www.CivileJournal.org

Civil Engineering Journal

(E-ISSN: 2476-3055; ISSN: 2676-6957)

Vol. 12, No. 04, April, 2026

Comparative Study of Crack Width Prediction Models for Reinforced Concrete Beams

Vlora Shatri [1], Burbuqe Shatri [1*], Armend Mujaj [1], Bajram Shefkiu [1]

[1] *Faculty of Civil Engineering, University of Prishtina, Prishtina 10000, Kosovo.*

Received 10 January 2026; Revised 10 March 2026; Accepted 17 March 2026; Published 01 April 2026

Abstract

Crack-width control is a critical serviceability limit state (SLS) requirement in reinforced concrete (RC) structures, as excessive cracking can compromise durability and accelerate reinforcement corrosion. This study evaluates the accuracy of crack width prediction models within major international design standards. An experimental investigation was conducted on a RC beam subjected to four-point bending, where crack propagation, beam deflections, and reinforcement stresses were monitored throughout the loading process. The measured crack widths were compared with analytical predictions from Eurocode 2 (EN 1992-1-1), DIN 1045-1, and ACI-based formulations. The results indicate that while all evaluated codes capture the general trend of increasing crack width with rising steel stresses under incremental loading, significant discrepancies exist in their predicted magnitudes. In general, it is Eurocode 2 that consistently provides the most conservative estimates, whereas DIN 1045-1 yields slightly lower but also consistent values of the same. Conversely, ACI-based approaches tend to underestimate crack widths at higher load levels. This study highlights the influence of modeling assumptions—specifically those related to bond-slip behavior, crack spacing, and tension stiffening—on the reliability of crack-width predictions. The results provide experimental evidence regarding the reliability and limitations of common predictive methods, contributing to a refined understanding of design rules for the serviceability of RC structures.

Keywords: Crack width; Serviceability Limit State; Reinforced Concrete Beam; Eurocode 2; DIN 1045-1; ACI 318; ACI 224.1R.

1. Introduction

Cracking is an inherent phenomenon in reinforced concrete (RC) structures, occurring once tensile stresses exceed the tensile strength of concrete. Although cracking does not necessarily compromise structural safety, excessive crack widths may significantly reduce durability, accelerate reinforcement corrosion, and negatively affect serviceability and aesthetics. Permissible crack widths in reinforced concrete structures are typically limited to about 0.1–0.4 mm, depending on environmental exposure and durability requirements, and modern structural design codes therefore include provisions aimed at controlling crack widths at the serviceability limit state (SLS).

Several international design standards provide analytical or empirical procedures for estimating crack widths in reinforced concrete members. Among the most widely applied are Eurocode 2 (EN 1992-1-1) [1], DIN 1045-1 [2], and the American standards ACI 318 [3] and ACI 224.1R [4]. These approaches differ substantially in their theoretical background and modeling assumptions. Eurocode-based formulations rely on mechanically derived relationships that incorporate bond interaction and tension stiffening effects, whereas ACI-based approaches are largely empirical expressions derived from regression analysis of experimental observations.

* Corresponding author: burbuqe.shatri@uni-pr.edu

https://doi.org/10.28991/CEJ-2026-012-04-019

© 2026 by the authors. Licensee C.E.J, Tehran, Iran. This article is an open access article distributed under the terms and conditions of the Creative Commons Attribution (CC-BY) license (http://creativecommons.org/licenses/by/4.0/).

A considerable amount of research has been devoted to modeling crack formation and crack-width development in reinforced concrete members. Several experimental studies have investigated crack width development in reinforced concrete beams [5–7]. Analytical models based on the compatibility of stresses and strains were proposed by Kaklauskas (2004) [8], providing a theoretical framework for predicting crack development in RC elements. More recently, improved analytical formulations have been proposed to better represent tension stiffening and stress transfer mechanisms in cracked reinforced concrete members. For example, Sakalauskas & Kaklauskas (2023) [9] introduced a refined analytical model for crack-width prediction based on improved mechanical representation of stress transfer between reinforcement and surrounding concrete.

In addition to analytical modeling approaches, several recent studies have evaluated the performance of crack-width prediction models implemented in international design codes. For instance, Van der Esch et al. (2024) [10] analyzed several crack-width formulations and demonstrated that different design standards may produce significantly different predictions depending on reinforcement configuration, concrete cover, and stress levels. Similar observations have been reported in other comparative investigations of international design codes.

Despite the considerable research devoted to crack-width prediction, discrepancies between theoretical predictions and experimental measurements continue to be reported in the literature [8]. Many previous studies focus either on analytical comparisons of design code provisions or on numerical modeling of cracking behavior [10, 11]. More recent analytical and experimental investigations have also highlighted the importance of accurately representing stress transfer mechanisms in reinforced concrete members [9, 12]. However, direct experimental comparisons of crack-width predictions obtained from different international design codes under identical boundary conditions remain relatively limited in the literature.

Therefore, further experimental validation of crack-width prediction models remains necessary in order to assess the reliability and applicability of existing design provisions used in structural engineering practice. The objective of this study is to evaluate the accuracy of crack-width prediction models implemented in Eurocode 2, DIN 1045-1, and ACI-based formulations through a combined experimental, analytical, and numerical investigation of a reinforced concrete beam subjected to four-point bending. The experimentally measured crack widths are compared with analytical predictions obtained from the different design codes and with results from numerical modeling, allowing a comprehensive assessment of the accuracy and conservativeness of the considered crack-width prediction approaches.

2. Research Methodology

The overall research methodology adopted in this study is illustrated in Figure 1.

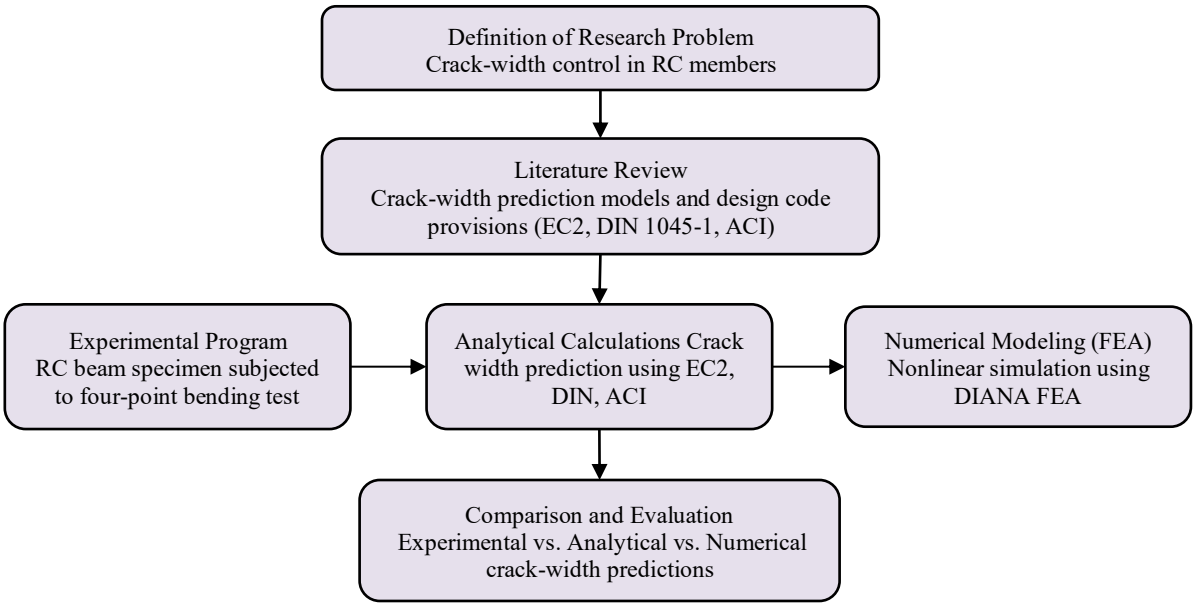

Figure 1. Flowchart illustrating the research methodology adopted in this study

3. Background on Flexural Cracking and Tension Stiffening

3.1. A Stages of Flexural Cracking in Reinforced Concrete Members

As illustrated in Figure 2, flexural cracking occurs when the tensile stress at the extreme tension fiber exceeds the concrete tensile strength, f_{ctm} [13]. Prior to cracking (Stage I), the concrete and reinforcement jointly resist tensile forces; the section exhibits linear elastic behavior, assuming that plane sections remain plane.

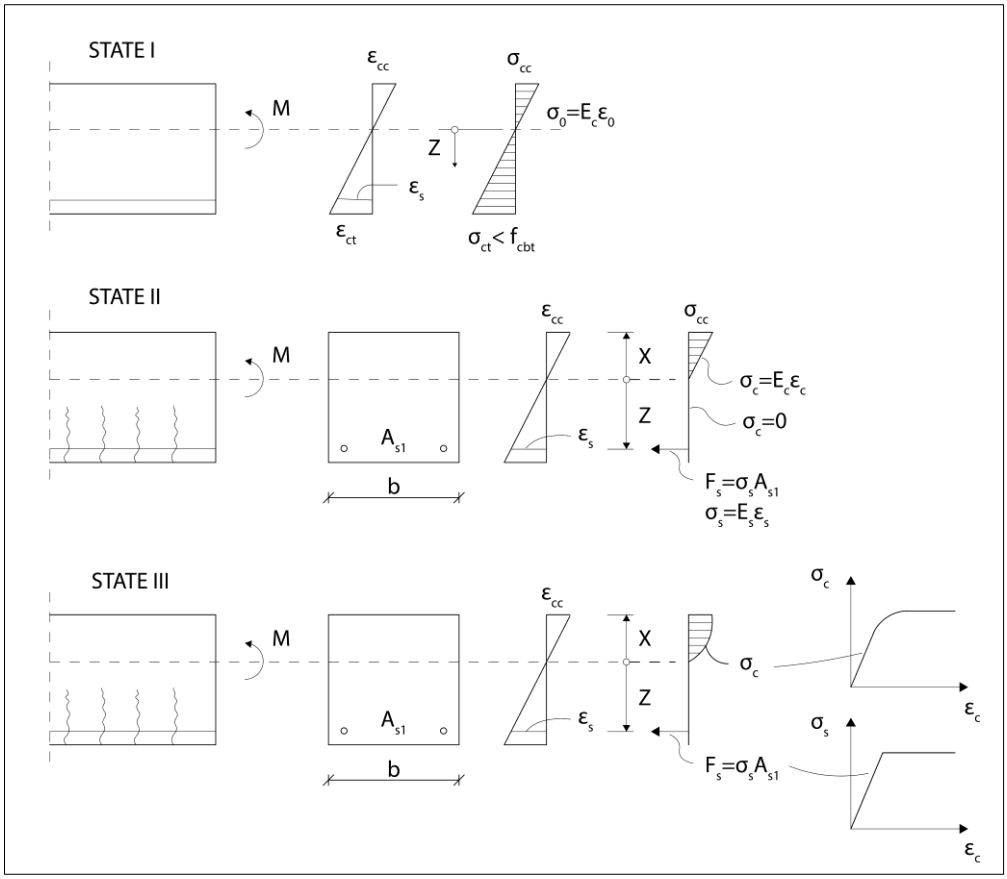

Figure 2. Behavioral stages of a reinforced concrete beam (after Engström 2015 [14])

Following the initiation of cracking, distributed micro-cracks develop and subsequently localize into discrete flexural cracks that propagate from the tension face toward the neutral axis (stage II). At crack locations, tensile stresses in concrete are effectively relieved, and reinforcement carries the entire tensile force. Between adjacent cracks, tensile stresses are partially transferred from reinforcement back to surrounding concrete through an interfacial bond, producing the tension-stiffening effect and resulting in nonlinear moment–curvature behavior.

As the load increases, the tensile reinforcement yields, accompanied by nonlinear compressive behavior of concrete (stage III). Ultimate failure occurs when the compression zone crushes at the ultimate bending moment (stage IV). From a serviceability perspective, structural performance is primarily governed by the stabilized cracking phase within stage II, where crack spacing becomes relatively uniform and crack widths can be meaningfully evaluated [15-17].

3.2. Parameters Influencing Crack Width and Tension Stiffening

During the stabilized cracking stage, crack width is influenced by several interrelated parameters, including:

- Steel stress under service loading,
- Reinforcement diameter and spacing,
- Concrete cover and effective tension area, and
- Bond interaction between steel reinforcement and surrounding concrete.

The contribution of concrete between cracks through bond interaction leads to tension stiffening, which reduces steel strain relative to a fully cracked section and plays a key role in controlling crack widths. Accurate modeling of this mechanism is therefore essential for reliable crack-width prediction [18].

Eurocode-based models explicitly incorporate these parameters through bond–slip-based formulations for crack spacing and crack width prediction. The effective reinforcement ratio and concrete cover are used to calculate the effective concrete area, which determines the extent of tension stiffening between cracks.

In contrast, ACI 318 has historically relied on semi-empirical expressions, most notably the Gergely–Lutz relationship, developed from regression analysis of experimental crack-width observations. While computationally simpler, these formulations do not explicitly model bond–slip behavior and tension stiffening, leading to differences in predicted crack widths when compared with Eurocode-based approaches.

4. Literature Review and Comparison with Previous Research

A substantial body of research has investigated crack formation and crack-width prediction in reinforced concrete (RC) members. Early studies focused on the fundamental relationship between reinforcement strain, bond behavior, and crack spacing. Beeby (1979, 2004) [19, 20] demonstrated that classical crack-spacing relationships of the form $s_r \propto \phi/\rho_{eff}$ often poorly correlate with experimental data unless the effects of concrete cover and bond characteristics are explicitly considered. These findings significantly influenced the development of Eurocode-style formulations based on effective reinforcement ratios and cover-dependent coefficients.

Carino & Clifton (1995) [17] provided a comprehensive review of cracking mechanics and code-based approaches, highlighting the limitations of purely empirical formulations and emphasizing the importance of consistent modeling of tension stiffening and bond behavior. Kattilakoski (2013) [21] conducted a systematic comparison of the provisions of Eurocode 2, ACI 318, and DIN 1045-1 using representative beam and slab examples. The study showed that EC2 and DIN generally provide similar and slightly conservative crack-width predictions, whereas ACI 318 may allow larger crack widths for comparable reinforcement layouts, particularly when crack control relies mainly on bar-spacing limitations.

Recent research has continued to evaluate and improve crack-width prediction models, including unified formulations for their prediction [22]. Liu & Lu (2024) [23] compared crack-width predictions across ACI 318, Eurocode 2, and the Chinese design code GB 50010. Their results found that while the overall development trends are similar, noticeable differences persist due to variations in theoretical assumptions and calculation procedures.

Several studies have also investigated the performance of different crack-width formulations implemented in international design standards. Van der Esch et al. (2024) [10] and Terjesen et al. (2024) [24] evaluated multiple crack-width calculation models, including those of Eurocode 2 and fib Model Code 2010 [25]. Their results indicated that no single method consistently provides accurate predictions for all geometries and reinforcement configurations. In particular, EC2 may overestimate crack widths in some cases and underestimate them in others, especially for members with large bar diameters and thick concrete covers.

In addition to code-based comparisons, several researchers have proposed improved analytical and numerical models to better represent the cracking behavior of reinforced concrete. Kaklauskas (2004) [8] developed an analytical crack model based on the compatibility of stresses and strains in cracked RC members, incorporating tension stiffening effects. More recently, Sakalauskas & Kaklauskas (2023) [9] proposed an analytical formulation for crack-width estimation that emphasizes the role of stress transfer mechanisms between reinforcement and surrounding concrete. Other studies have investigated the influence of reinforcement ratio and concrete cover on crack development. Experimental research by Sokolov et al. (2025) [12] confirmed the significant role of reinforcement configuration and bond interaction in controlling crack spacing and crack width.

Recent developments have also explored advanced modeling techniques. Gribniak et al. (2024) [18] investigated improved tension-stiffening models and showed that more accurate representation of concrete–steel interaction significantly improves crack-width predictions. Numerical approaches have also been applied to simulate crack development in reinforced concrete structures. Červenka et al. (2025) [13] demonstrated that nonlinear finite element models are capable of reproducing crack localization and propagation under increasing load.

Recent studies have introduced data-driven approaches for crack-width prediction in reinforced concrete beams, with machine-learning techniques demonstrating improved predictive capability compared to traditional empirical models [26, 27]. Despite extensive research on crack-width prediction, discrepancies between theoretical models and experimental data are frequently reported in literature. Many studies focus either on analytical comparisons of design-code provisions or on numerical modeling of cracking behavior. However, relatively few investigations integrate experimental testing, analytical code-based evaluation, and numerical simulation under identical boundary conditions.

Therefore, further experimental validation of crack-width prediction models is essential to assess their reliability and applicability in practical structural design. This study contributes to the field through a combined experimental, analytical, and numerical investigation of crack-width development in a reinforced concrete beam subjected to four-point bending. Measured crack widths are compared against predictions from Eurocode 2, DIN 1045-1, and ACI-based formulations, providing a comprehensive evaluation of the accuracy and conservatism of these diverse modeling approaches.

5. Crack Width Prediction According to Design Codes

5.1. Eurocode 2 (EN 1992-1-1, 2004)

Eurocode 2 [20] evaluates the characteristic crack width w_k as:

$$w_k = s_{r.max} \cdot (\varepsilon_{sm} - \varepsilon_{cm}) \quad (1)$$

where, $s_{r,max}$ = maximum crack spacing, ε_{sm} = mean steel strain, and ε_{cm} = mean concrete strain between cracks.

The strain difference ε_{sm}- ε_{sm} can be expressed as:

$$\varepsilon_{sm} - \varepsilon_{cm} = \frac{\sigma_s - k_t \frac{f_{ct.eff}}{\rho_{p.eff}} \cdot (1 + \alpha_e \cdot \rho_{p,eff})}{E_s} \geq 0{,}6 \frac{\sigma_s}{E_s} \quad (2)$$

where, σ_s is the stress in the tensile reinforcement in a cracked section: $\sigma_s = M/(A_s \cdot z)$, in which M is the bending moment, A_s is the area of reinforcing steel within the tensile zone, and z is the lever arm of internal forces; α_e is the ratio E_s / E_{cm}, where E_s is the modulus of elasticity of the steel reinforcement and E_{cm} is the mean modulus of elasticity of the concrete; k_t is a factor dependent on the load duration: $k_t = 0.6$ for short-term loading and $k_t = 0.4$ for long-term loading; $\rho_{p,eff}$ is the effective reinforcement ratio: $\rho_{p,eff} = (A_s + \xi_1 A'_p)/A_{c,eff}$, where A_p' is the area of pre- or post-tensioned tendons within $A_{c,eff}$; $A_{c,eff}$ is the effective area of concrete in tension: $A_{c,eff} = b \cdot h_{c,eff}$ where b is the section width and h_{ceff} is the effective height, taken as the minimum of *2.5(h-d), (h-x)/3, or h/2* (see Figure 3); ξ_1 is the adjusted bond strength ratio accounting for different diameters of prestressing and reinforcing steel: $\xi_1 = \sqrt[2]{\xi \, \phi_s / \phi_p}$, where ξ is the ratio of bond strength of prestressing and reinforcing steel, ϕ_s is the largest bar diameter of reinforcing steel, ϕ_p is the equivalent diameter of tendon.

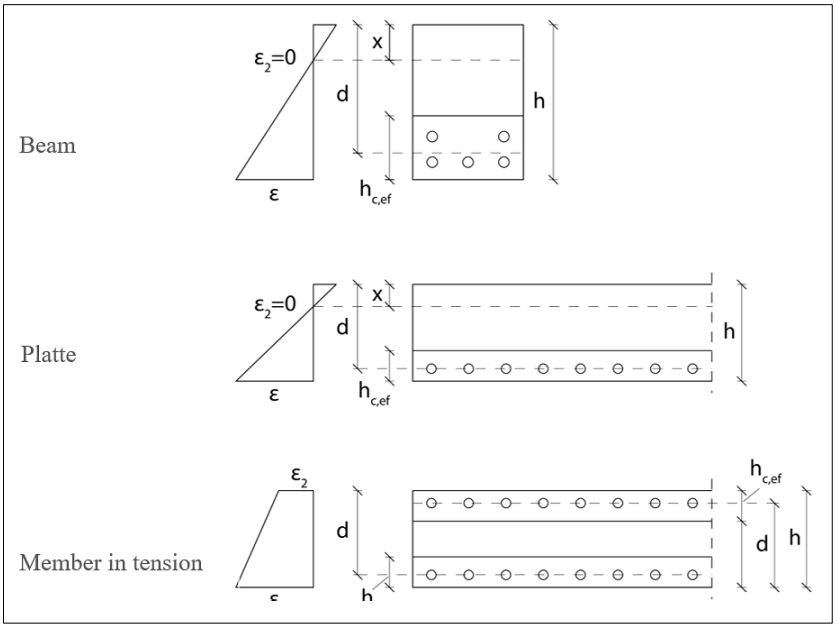

Figure 3. Effective tension area in reinforced concrete members: typical cases according to EN 1992-1-1 (2004) [20]

It is a characteristic of individual cracks that the strains in the reinforcement and concrete at the ends of the maximum crack spacing are equal (see Figure 4).

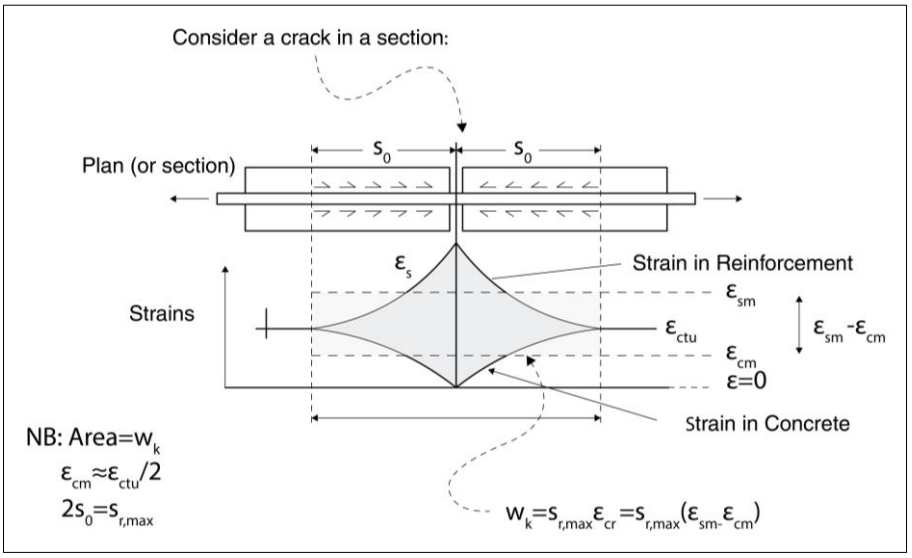

Figure 4. Strain distribution in concrete and reinforcement at individual cracks according to practical design provisions of Eurocode 2 (EN 1992-1-1, 2004) [1]

The maximum crack spacing depends on the reinforcement layout. When bars are closely spaced ($s \leq 5(c + \phi/2)$), the maximum spacing is given by:

$$s_{r.max} = k_3 \cdot c + k_4 \cdot k_1 \cdot k_2 \cdot \phi/\rho_{eff} \quad (3)$$

where c is the concrete cover; ϕ is the bar diameter; k_1 is a coefficient reflecting the bond properties of the reinforcement: $k_1 = 0.8$ for high bond (deformed) bars and $k_1 = 1.6$ for smooth bars; k_2 is a coefficient representing the strain distribution across the section: $k_2 = 0.5$ for member in pure bending and $k_2 = 1.0$ for sections in axial tension section; k_3 *and* k_4 are constants, typically taken as *3.4 and 0.425*, respectively; $\rho_{p,eff}$ is the effective reinforcement ratio. When the bar spacing exceed $5(c + \phi/2)$, (see Figure 5) the maximum crack spacing is approximated as:

$$s_{r.max} = 1{,}3 \cdot (h - x) \quad (4)$$

where, x is the neutral axis depth and h is the overall depth of the cross-section.

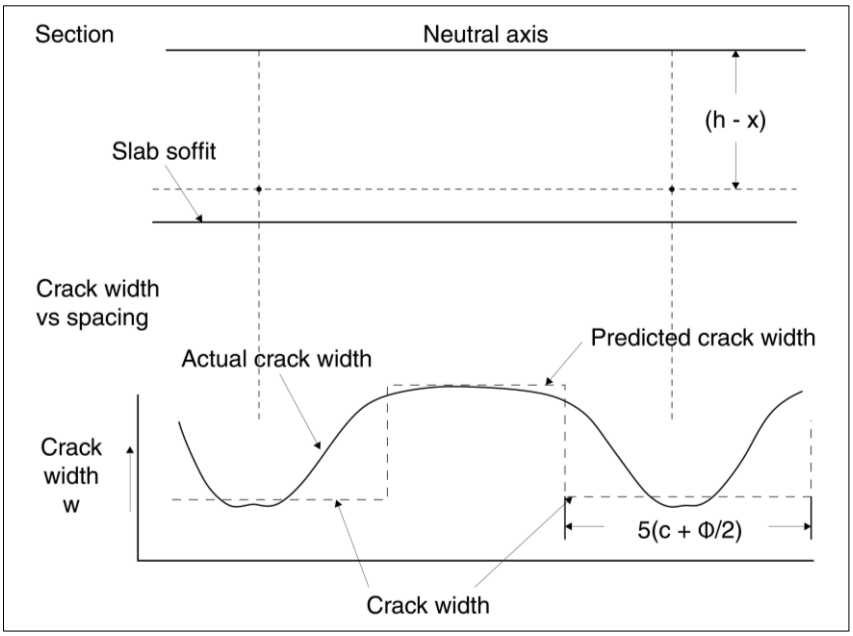

Figure 5. Maximum crack width, *w*, at the concrete surface as a function of the distance from the reinforcing bar (EN 1992-1-1, 2004) [1]

Concrete tensile strength contributes to the structural response through tension stiffening, which is accounted for by using reduced steel stresses in the cracked section. EN 1992-1-1 specifies limiting crack widths based on the exposure class (typically 0.1–0.4 mm).

5.2. DIN 1045-1

DIN 1045-1 [2] adopts a conceptually similar formulation to Eurocode 2, also basing crack spacing on the effective reinforcement ratio and concrete cover, with coefficients calibrated from German experimental data [28]. Certain provisions allow for indirect crack control solely via bar spacing, particularly for members in moderate exposure classes. Alternatively, the crack width limitation can be verified by direct calculation using Equation 1. The maximum crack spacing may be calculated according to Equation 5:

$$s_{r.max} = \phi/(3{,}6 \cdot \rho_{eff}) \leq \sigma_s \cdot \phi/(3{,}6 \cdot f_{ct.eff}) \quad (5)$$

where, $s_{r,max}$ is the maximum distance between two consecutive cracks; $f_{ct,eff}$ is the effective tensile strength of concrete (often taken as the mean tensile strength, f_{ctm}); σ_s is reinforcement stress at the crack location; ϕ is the bar diameter; $\rho_{p,eff}$ is the effective reinforcement ratio, defined as $\rho_{p,eff} = (A_s + \xi_1^2 A'_p)/A_{c,eff}$ (as in EC-2 [1]).

The difference between the mean strains of the concrete and reinforcing steel is calculated as follows:

$$\varepsilon_{sm} - \varepsilon_{cm} = \frac{\sigma_s - 0{,}4\frac{f_{ct.eff}}{\rho_{eff}} \cdot (1 + \alpha_e \cdot \rho_{eff})}{E_s} \geq 0{,}6\frac{\sigma_s}{E_s} \quad (6)$$

where, σ_s is the reinforcement stress at the crack location; α_e is the modular ratio, defined as E_s / E_{cm}, where E_s is the modulus of elasticity of the steel reinforcement and E_{cm} is the mean modulus of elasticity of the concrete.

Unlike EC2, the DIN formulations do not explicitly consider load duration; a single factor of 0.4 is applied.

5.3. ACI 318 and ACI 224.1R

Historically, the ACI approach uses the Gergely–Lutz equation, an empirical expression derived from over 900 experimental crack measurements in beams [3, 29].

For members in bending, the maximum crack width is calculated as:

$$w_{max} = 11{,}0 \cdot \frac{h_2}{h_1} \cdot \sigma_s \cdot \sqrt[3]{A \cdot d'} \cdot 10^{-6}\ (mm) \tag{7}$$

where σ_s is the steel stress at the crack location (N/mm^2); h_1 the distance of the neutral axis to the centroid of the tensile reinforcement (mm); h_2 is the distance from the neutral axis to tension face (mm) (see Figure 6); A is the effective tensile cross-sectional area per bar (mm^2), defined as $A=2bc/n_s$ for members in bending, where n_s is the number of reinforcing bars in the tensile zone; For pure tension, $A = 2d's$, where $d'$is the distance from the centroid of the first bar row of bars to the tension edge (mm) and s is the reinforcement spacing (mm).

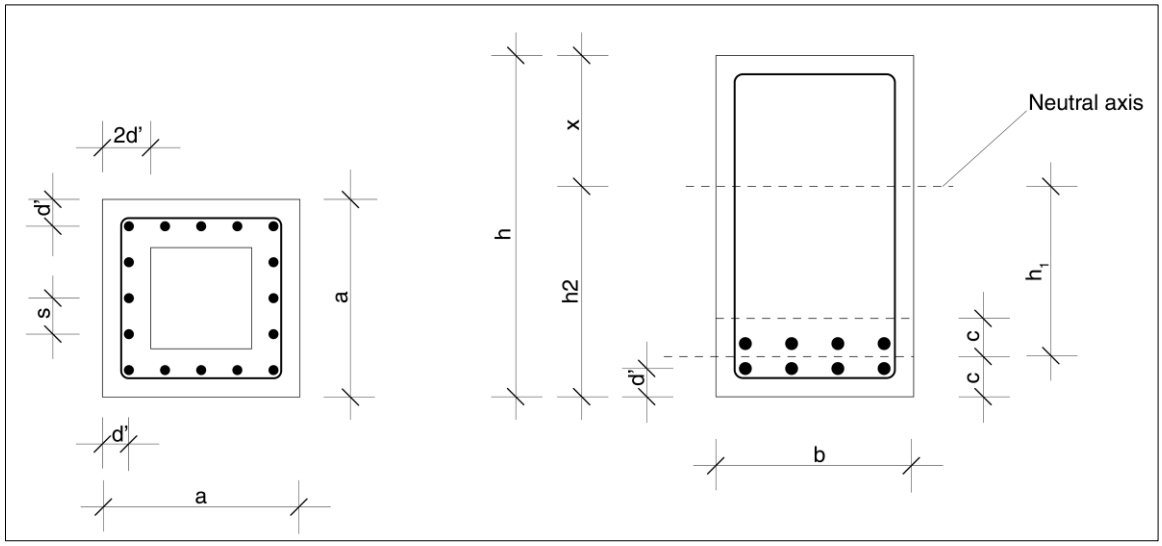

Figure 6. Examples for determining the effective tension area (adapted from EN 1992-1-1 [1])

For comparison with the EC2 predictions, the mean crack width is modified as follows:

$$w_{max} = 8.3 \cdot \frac{h_2}{h_1} \cdot \sigma_s \cdot \sqrt[3]{A \cdot d'} \cdot 10^{-6}\ (mm) \tag{8}$$

The characteristic crack width according to EN 1992-1-1 is expressed as:

$$w_k = \beta \cdot w_m \leq w_g \tag{9}$$

where β is a coefficient that accounts for the load type: β = 1.7 for imposed loads and β = 1.3 for imposed deformation; w_m is the mean crack width; w_g is the limiting crack width.

Later versions of ACI 318 emphasize indirect crack control via bar spacing and steel stress limits under service loads. However, ACI 224.1R continues to provide explicit formulas for maximum crack width:

$$w = 2 \cdot \frac{\sigma_s}{E_s} \cdot \beta \cdot \sqrt[2]{{d_c}^2 + \left(\frac{s}{2}\right)^2} \tag{10}$$

where d_c is the concrete cover thickness to the centre of the nearest bar (mm); s is the bar spacing (mm); β is the ratio of the distance from the neutral axis to the centroid of the reinforcing steel.

Compared to EC2 and DIN, ACI formulas are simpler and involve fewer parameters, though they are less directly linked to mechanical bond–slip models. The empirical nature of ACI formulations has been discussed in previous studies [30].

6. Evaluation of Crack Width Predictions According to Design Codes

To assess the accuracy of crack-width prediction models, analytical calculations were performed in accordance with the Eurocode 2 (EN 1992-1-1), DIN 1045-1, and ACI-based formulations. These standards employ distinct theoretical frameworks for estimating crack widths in reinforced concrete members. While Eurocode 2 and DIN 1045-1 rely primarily on mechanically- based models that integrate parameters such as effective tension area, reinforcement ratio, and crack spacing, the ACI approach is primarily based on empirical relationships derived from experimental data.

Calculations were performed using the actual geometry and reinforcement configuration of the tested reinforced concrete (RC) beam (as detailed in Table 2 and Figure 8). Material properties obtained from experimental testing- conducted in accordance with BS EN 12390-2:2019 [31, 32] - were adopted in the analytical evaluation to ensure consistency across the experimental, analytical, and numerical phases of the study.

Table 1 summarizes the predicted crack widths according to Eurocode 2, DIN 1045-1, and ACI formulations across various load levels. Significant discrepancies in the magnitude of predicted crack widths are observed, stemming from differing assumptions regarding bond behavior, crack spacing, and tension stiffening.

DIN 1045-1 yields crack-width predictions that align closely with those of Eurocode 2, though they remain consistently lower across the investigated load range. This similarity reflects the shared theoretical framework of both standards and their calibration against comparable experimental datasets.

In contrast, ACI-based formulations exhibit a distinct trend. The Gergely–Lutz model, as adopted in ACI 224.1R, provides crack-width values that correlate well with experimental measurements at moderate load levels but becomes progressively less conservative as the load increases. This behavior is attributed to the semi-empirical nature of the model and its simplified treatment of bond- slip interaction and crack spacing, resulting in lower predicted values compared to the Eurocode and DIN approaches at higher steel stress levels.

Overall, Eurocode 2 provides the most conservative crack-width predictions within the investigated range, while DIN 1045-1 produces slightly lower but consistent values. ACI-based methods offer simpler computational procedures but tend to underestimate crack widths under higher service load conditions.

As shown in Table 1, the predicted crack width according to Eurocode 2 reaches 0.396 mm at a load level of 65 kN, which is nearly identical to the commonly adopted serviceability limit of 0.4 mm for reinforced concrete members. This load level, therefore, represents a critical service state for crack-width control in the investigated beam.

Table 1. Summary of applied load levels, steel stresses, strain differences, crack spacings, and predicted crack widths according to Eurocode 2, DIN 1045-1, and ACI formulations

P [kN]	σ_s [MPa]	$(\varepsilon_{sm} - \varepsilon_{cm}) \times 10^{-3}$ [EC 2]	$s_{r,max}$ [EC 2] [mm]	w_k[EC 2] [mm]	w_k[DIN 1045] [mm]	w_k [ACI 213] [mm]	w_k[ACI 224.1R] [mm]
15 kN	135.69	0.4081	144.66	0.086	0.0573	0.0815	0.06
30 kN	233.73	0.7942	144.66	0.136	0.115243	0.1400	0.114
40 kN	299.04	1.1219	144.66	0.193	0.156283	0.1798	0.145
50 kN	364.45	1.4495	144.66	0.249	0.1973	0.2190	0.177
60 kN	429.81	1.777	144.66	0.362	0.2384	0.2584	0.209
65 kN	462.49	1.941	144.66	0.396	0.259	0.2780	0.225
70 kN	495.17	2.1048	144.66	0.431	0.2794	0.2980	0.241
75 kN	527.85	2.269	144.66	0.465	0.299	0.3173	0.257
79 kN	554.00	2.40	144.66	0.492	0.3163	0.3330	0.27

The variation of predicted crack widths under incremental loading is illustrated in Figure 7. All considered design codes demonstrate a gradual increase in crack width in response to rising load level and steel stresses.

The trends observed in Figure 7 are consistent with findings reported in previous studies. Comparative analyses between Eurocode- and ACI-based crack-width predictions have similarly shown that Eurocode formulations generally provide more conservative estimates, while ACI-based approaches tend to predict smaller crack widths at higher load levels [8, 9, 12].

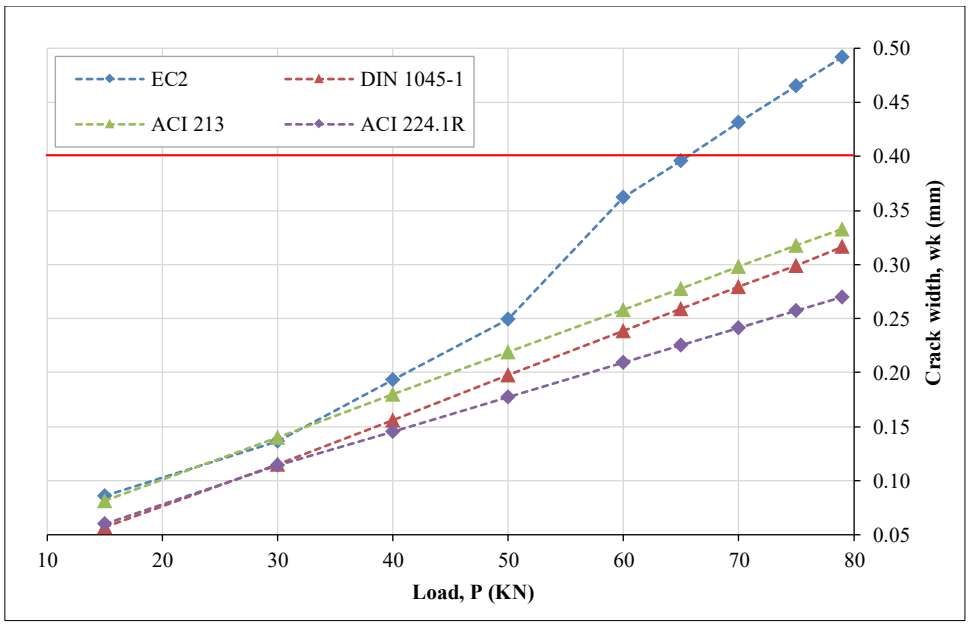

Figure 7. Comparison of predicted crack-width according to various design standards

These analytical results establish the foundation for the comparative analysis with the experimentally measured crack widths presented in the subsequent section.

7. Experimental Program

7.1. Specimen and Materials

The experimental investigation was conducted on a reinforced concrete (RC) beam designed to evaluate crack-width development under four- point bending. The geometric properties and reinforcement details are summarized in Table 2, with the reinforcement layout illustrated in Figure 8.

Table 2. Geometric properties and reinforcement details of the tested RC beam

Beam ID	L (mm)	L_{eff} (mm)	h (mm)	b (mm)	c (mm)	A_{sl}	A_{sl}'	A_{sw}
C 30-1	5000	4800	400	200	20	4ϕ12	2ϕ10	Φ8@20

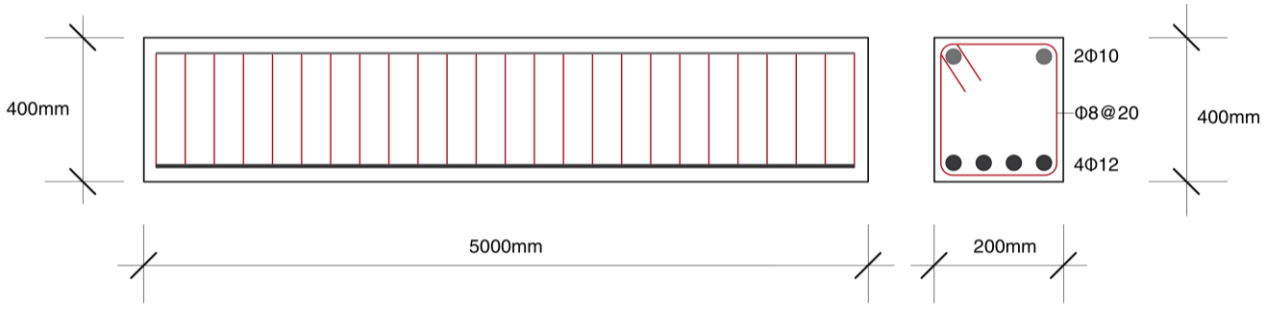

Figure 8. Geometry and reinforcement layout of the tested RC beam

The beam had a total length of 5000 mm and an effective span of 4800 mm, with a rectangular cross-section of 200 mm × 400 mm and a concrete cover of 20 mm. Longitudinal reinforcement consisted of four Ø12 tension bars and two Ø10 compression bars, while Ø8 stirrups spaced at 200 mm provided transverse reinforcement.

The beam was cast using normal-weight concrete with a nominal design strength corresponding to class C30/37. These design properties were adopted for the analytical and numerical calculations as presented later in this study.

To verify the material properties, concrete specimens were tested in accordance with BS EN 12390-2:2019 [31]. The mechanical properties obtained from the compression testing are summarized in Table 3. The results indicate that the average 28- day compressive strength slightly exceeded the characteristic value for class C30/37, confirming that the concrete satisfied the design requirements.

Table 3. Mechanical properties of the concrete specimens sampled from the RC beam [31, 32]

Sample No.	Apparent density (kg/m³)	Age (days)	Maximum load (kN)	Cross-sectional area (mm²)	Compressive strength (MPa)
M-1	2420	2	569.3	22500	25.30
M-2	2420	2	553.5	22500	24.60
Average	**2420**		**561.4**		**24.95**
M-3	2430	7	803.3	22500	35.70
M-4	2420	7	814.5	22500	36.20
Average	**2420**		**809.0**		**35.95**
M-5	2440	28	985.5	22500	43.80
M-6	2440	28	956.3	22500	42.50
M-7	2440	28	913.5	22500	40.60
Average	**2430**		**951.80**		**42.30**

For the longitudinal reinforcement, Grade 500 steel bars were utilized. Tensile tests were performed per ISO 15630-1:2019 [33] to determine key mechanical properties, including yield strength (f_y), ultimate tensile strength (f_u), modulus of elasticity (E_s), and the ductility ratio. These experimentally determined properties are presented in Table 4.

Table 4. Mechanical properties of the steel reinforcement [33]

	Diameter (mm)	Length (mm)	Cross-sectional Area (mm²)	Mass (kg)	Ultimate Tensile Strength, f_t (MPa)	Yield Strength, f_y (MPa)	Ductility Ratio $k=f_t/f_y$	Modulus of Elasticity, E (MPa)
	8.05	559	51.10	0.22	598.4	515.9	1.16	198254
M-1	8.01	557	50.20	0.22	598.7	525.2	1.14	200453
	8.06	558	51.20	0.22	592.0	514.8	1.15	199476
	12.02	548	112.7	0.49	679.3	585.6	1.16	199858
M-2	11.98	547	112.8	0.49	672.9	585.1	1.15	198487
	11.97	554	112.5	0.49	680.6	586.7	1.16	201365

The geometry, material properties, and reinforcement configuration described above served as the primary input parameters for the analytical crack-width calculations and numerical modeling presented in the following sections.

7.2. Test Setup and Instrumentation

The reinforced concrete (RC) beam was subjected to four-point bending, with two equal concentrated loads applied symmetrically about the mid-span (Figure 9). This configuration established a constant moment region in the central portion of the beam, facilitating crack development within the pure bending zone while minimizing shear influence.

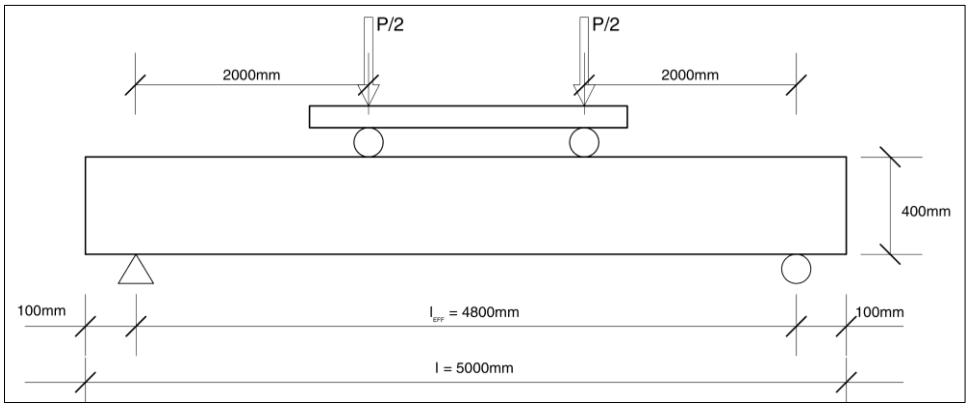

Figure 9. Four-point bending test configuration of the RC beam

Testing was conducted using a displacement-controlled hydraulic actuator, with the load increased quasi-statically from 15 kN to 79 kN. Linear Variable Differential Transformers (LVDTs) and strain gauges were installed at selected locations to monitor deflections and strains throughout the loading process (Figure 10). Specifically, LVDTs measured vertical displacements, while strain gauges were bonded to the reinforcement and concrete surfaces to record strain evolution.

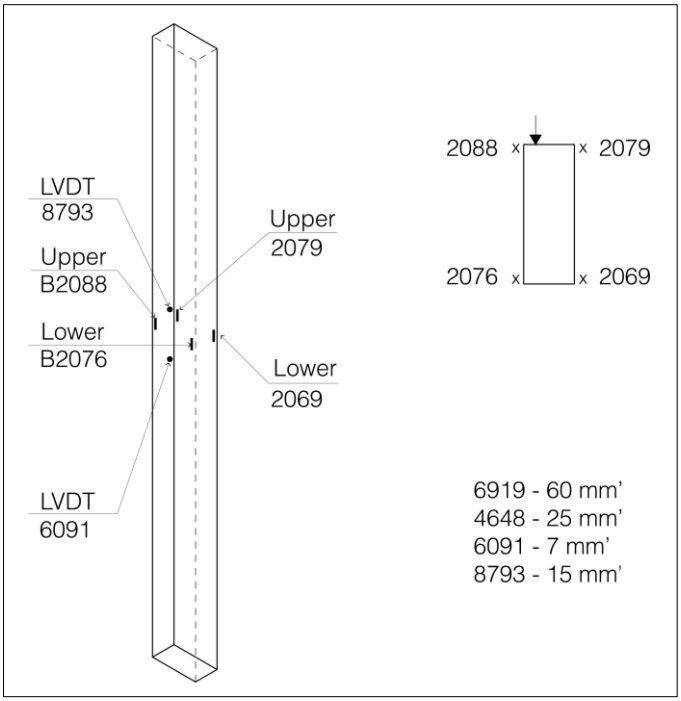

Figure 10. Instrumentation layout: LVDT and strain gauge positions for measuring deflection and strain in the RC beam

Crack widths were measured using a mechanical crack gauge throughout the loading process. Measurements were taken at predefined load levels once each increment had stabilized. The gauge provided accuracy of approximately 0.01 mm, enabling precise monitoring of crack development within the tensile zone.

Measurements were concentrated at the most critical cracks within the constant moment region between the loading points. Particular attention was directed toward cracks exhibiting the widest openings. At each load level, the maximum crack width (w_{max}) was recorded to facilitate a direct comparison with width predictions from Eurocode 2, DIN 1045-1, and ACI formulations.

The experimental setup and the condition of the beam during the loading stage are shown in Figure 11. Figure 11-a presents a general view of the four-point bending test configuration, while Figure 11-b provides a detailed view of the beam under load. This close-up highlights the flexural crack development in the tension zone and the LVDT instrumentation used for monitoring.

(a) (b)

Figure 11. Experimental setup and crack development in the tested RC beam under four-point bending: (a) general view of the test configuration; (b) detailed view of crack formation and instrumentation (LVDTs)

7.3. Loading System

The vertical load was applied via a hydraulic actuator positioned between the steel reaction frame and the beam's top surface, as shown in Figure 12-a. A pressure gauge (see Figure 12-b) enabled continuous monitoring of the applied force. The system was precisely aligned to avoid eccentricities, ensuring concentric load transmission.

(a) (b)

Figure 12. Hydraulic loading system: (a) Hydraulic jack; (b) Pressure gauge for controlled load application

Beneath the loading points, the support conditions and guiding systems maintained stable contact, while LVDTs recorded vertical displacements in real time. This configuration ensured that:

- The load was applied incrementally in a high controlled manner.
- Force measurements were direct, ensuring high reliability throughout the testing range.
- Beam displacements and deflections were accurately captured.
- The structural response accurately reflected the inherent beam behavior rather than apparatus interference or experimental limitations.

7.4. Crack Measurement

Crack widths were measured directly during the test using a Elco meter 143 Crack Width Ruler. Figure 13-a illustrates an in-situ measurement at an applied load of 40 kN, showing a crack width of approximately 0.15 mm. Figure 13-b provides a closer view of vertical flexural cracks in the tension zone, depicting the characteristic cracking pattern under flexural loading.

(a) (b)

Figure 13. Measurement of crack width: (a) In-situ crack gauge measurement at 40 kN; (b) Detail view of vertical flexural cracks in the tension zone

The observed cracks were predominantly vertical, propagating from the extreme tension fiber toward the neutral axis. This behavior confirms the tensile activation of the concrete and effective bond-stress transfer to the reinforcement. At the 40 kN load level, the measured crack width (~0.15 mm) remained well within the serviceability limit state of 0.2–0.4 mm. This indicates a controlled nonlinear-elastic response prior to reaching critical stress levels. Figures 14 and 15 illustrate the global crack distribution and the fracture morphology at higher load increments.

Figure 14. Crack distribution and final state of the RC beam following the experimental test

Figure 15. Crack distribution and failure locations at the ultimate load stage

8. Comparison of Crack Width Predictions with Experimental Measurements

Crack development was concentrated within the constant moment region of the beam. As the load increased, flexural cracks initiated in the tension zone and progressively widened during subsequent stages. These crack openings were monitored continuously, with discrete measurements recorded at predefined load levels.

Table 5 summarizes the experimental crack widths obtained during the test. At lower load levels (15–40 kN), crack widths remained minimal, representing the crack initiation phase. Beyond 50 kN, however, the openings increased significantly, driven by rising reinforcement stresses and stabilization of the crack pattern.

Table 5. Experimentally measured crack widths obtained during the loading test

P [kN]	$w_{k(exp)}$ [mm]
15 kN	0.00
30 kN	0.10
40 kN	0.15
50 kN	**0.25**
60 kN	**0.30**
65 kN	**0.33**
70 kN	0.35
75 kN	2.00
79 kN	N/A

Notably, the crack width of 2.00 mm recorded at 75 kN corresponds to the near-failure stage. This value exceeds typical serviceability conditions and instead reflects the structural response as the beam approaches its ultimate load capacity.

To evaluate the predictive accuracy of the various models, the experimental data were compared against the analytical estimates from Eurocode 2 (EN 1992-1-1), DIN 1045-1, and ACI formulations. The percentage performance deviation between the predicted ($w_{k,code}$) and experimental ($w_{k,exp}$) crack widths was calculated as follows:

$$\Delta = \frac{w_{k.code} - w_{k.exp}}{w_{k.exp}} \times 100 \quad (11)$$

where, $w_{k,code}$ is the predicted crack width obtained from the design code formulation; $w_{k,exp}$ is the experimentally measured crack width.

The calculated deviations are summarized in Table 6, while Figure 16 illustrates the comparison between predicted and experimentally measured crack widths across the investigated load levels.

Table 6. Percentage deviation of predicted crack widths relative to experimental measurements

P[kN]	$(w_{k[EC2]} - w_{k[exp]})/w_{k[exp]}$	$(w_{k[DIN]} - w_{k[exp]})/w_{k[exp]}$	$(w_{k[ACI\ 213]} - w_{k[exp]})/w_{k[exp]}$	$(w_{k[ACI\ 224]} - w_{k[exp]})/w_{k[exp]}$
15	N/A	N/A	N/A	N/A
30	+ 36.00 %	+ 15.24 %	+ 40.00 %	+ 14.00 %
40	+ 28.67 %	+ 4.1890 %	+ 19.87 %	− 3.333 %
50	− 0.400 %	− 21.080 %	− 12.40 %	− 29.20 %
60	+ 20.67 %	− 20.530 %	− 20.67 %	− 30.33 %
65	+ 21.09 %	− 21.52%	− 15.76 %	− 29.69 %
70	+ 23.14 %	− 72.06 %	− 14.86 %	− 31.14 %
75	− 76.75 %	− 85.00 %	− 84.14 %	− 87.15 %
79	N/A	N/A	N/A	N/A

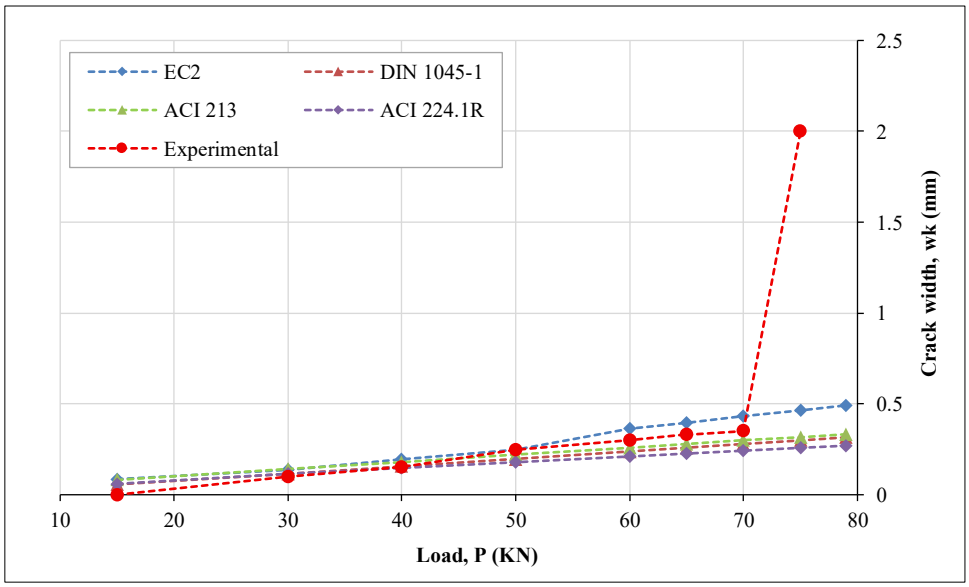

Figure 16. Comparison of predicted crack-widths from various design codes with experimental measurements

Figure 16 demonstrates that all evaluated design codes accurately capture the progressive increase in crack width as a function of load and reinforcement stress. However, significant discrepancies in the magnitude of predicted widths are evident, stemming from the divergent theoretical assumptions inherent in each formulation.

8.1. Eurocode 2 Prediction

Eurocode crack-width predictions show good agreement with experimental measurements, generally yielding slightly higher, conservative values. The model's mechanically based formulation, which integrates bond interaction, effective tension area, and crack spacing, tends to slightly overestimate crack widths compared to measured data. For example, at a load level of 50 kN, the predicted crack width is approximately 0.25 mm, which correlates closely to the experimentally measured value.

At lower load levels (30–40 kN), EC2 predicts crack widths in the range of 0.14–0.19 mm, whereas the measured values range between 0.10 and 0.15 mm. This tendency of EC2 to moderately overestimate crack widths is consistent with previous studies and reflects the mechanically based formulation of the Eurocode model, which integrates bond-slip interaction, effective tension area, and crack spacing.

8.2. DIN 1045-1 Predictions

The crack-width predictions obtained from DIN 1045-1 are generally consistent with those from Eurocode 2, although they tend to yield slightly lower values. This behavior reflects the shared theoretical framework of the two design standards.

Across most load levels, DIN 1045-1 predictions remain consistent with the experimental results, particularly within the serviceability range. The minimal deviations observed between DIN predictions and measured crack widths indicate that this formulation provides a reliable estimate for beams with conventional reinforcement ratios and typical concrete cover.

8.3. ACI-Based Predictions

The ACI-based crack-width formulations, particularly the Gergely–Lutz model adopted in ACI 224.1R, generally yield smaller crack-width values than the Eurocode-based approaches. While predicted crack widths are relatively consistent with experimental values at moderate load levels, the ACI formulations tend to underestimate crack widths as the load increases. This trend aligns with findings from previous studies evaluating code-based crack-width models [10, 22, 30].

For example, at 60 kN, the ACI-based prediction is approximately 0.26 mm, whereas the experimentally measured crack width is approximately 0.30 mm. This behavior can be attributed to the semi-empirical nature of the ACI formulations, which rely primarily on simplified relationships involving reinforcement spacing, concrete cover, and steel stress.

8.4. Overall Comparison of Code Performance

The comparison between analytical predictions and experimental measurements reveals three critical trends.

First, Eurocode 2 consistently yields the most conservative crack-width predictions, particularly as load levels increase. Second, DIN 1045-1 provides estimates that are slightly lower than those of Eurocode 2 but maintain a high correlation with experimental results. Third, ACI-based formulations tend to underestimate crack widths at higher load levels, reflecting the simplified empirical framework.

At the initial loading stages ($\leq$ 40 kN), all evaluated design codes accurately capture the general trend of crack formation. However, as the load and reinforcement stress increase, the discreoancies between the models become more pronounced. This behavior aligns with previous studies indicating that empirical formulations tend to underestimate crack widths compared to mechanically based models that explicitly account for bond interaction and tension stiffening [10, 22, 30].

In summary, the results demonstrate that Eurocode 2 and DIN 1045-1 offer more reliable crack-width predictions for the tested beam, as their formulations explicitly integrate bond behavior, effective tension area, and reinforcement distribution. Conversely, the simplified empirical relationships utilized in the ACI-based methods tend to underestimate crack widths as load levels increase, potentially overlooking critical serviceability conditions.

9. Numerical Model and Boundary Conditions

The numerical model was developed and analyzed using the DIANA FEA software [13], enabling a nonlinear simulation of reinforced concrete behavior through to failure. The beam was modeled as three-dimensional solid with uniform geometry, accurately reflecting the physical characteristics of the experimental specimen.

Discretization was achieved through a finite element mesh with density optimized to capture crack propagation, stress distribution, and strain localization. The mesh configuration was specifically refined to prevent numerical instabilities and to ensure convergence during the nonlinear analysis phase.

Boundary conditions were defined in DIANA FEA to replicate the experimental setup. One end support was modeled with restrained vertical displacement, while the opposite end was defined as a roller, permitting longitudinal movement. This configuration prevents the development of parasitic axial forces and ensures a realistic flexural response.

The load was applied incrementally through discrete analysis steps, replicating the quasi-static experimental procedure. In DIANA FEA, this incremental approach facilitates tracking of progressive behavior, spanning the elastic phase, crack initiation, and propagation, through to reinforcement yielding and ultimate structural failing.

Material modeling was performed by incorporating the nonlinear constitutive laws for both concrete and reinforcement, enabling an accurate reproduction of bond-slip interaction and the ductile failure mechanism. Consequently, the numerical model implemented in DIANA FEA is directly consistent with the experimental setup and is suitable for characterizing the beam's structural response up to failure.

9.1. Crack Modeling in DIANA FEA and Interpretation of Results

Numerical modeling was performed using a two-dimensional (2D) approach in DIANA FEA, where a nonlinear smeared crack model characterizes the tensile behavior of the concrete. In this framework, cracks are represented as distributed strain localizations within the finite elements rather than discrete physical discontinuities, accurately capturing the progressive stiffness degradation of the concrete post-cracking.

The Figure 17 illustrates the geometric and structural scheme of the beam, where the element is modeled as a continuous three-dimensional body with regular discretization. The boundary conditions are defined as follows:

- Fixed support restricting both vertical and horizontal displacements at one end to replicate a pinned connection, allowing for rotation while preventing translation;
- Sliding support restricting the vertical displacement at the opposite end while permitting longitudinal movement to simulate a roller support, which prevents the development of parasitic axial forces.
- The load is applied as a concentrated force in the upper zone of the beam, generating dominant positive bending consistent with the experimental four-point bending setup.

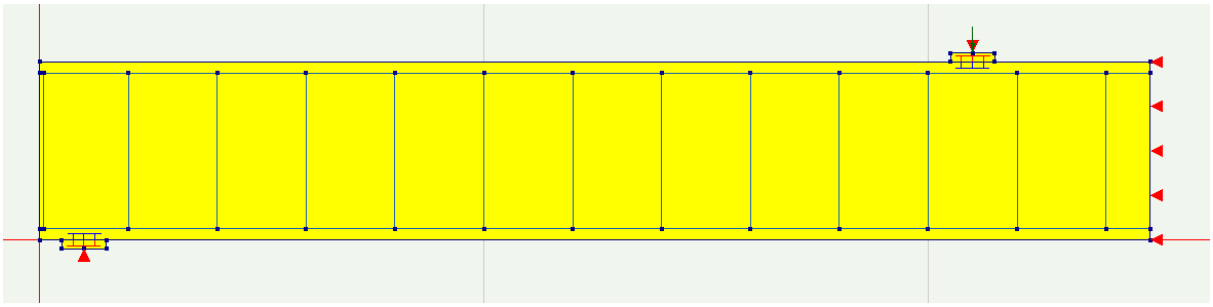

Figure 17. Two-dimensional geometric model of the reinforced concrete beam, illustrating boundary conditions loading points

The Figure 18 illustrates the mesh discretization of the model, featuring a dense and regular element distribution along the entire beam length to reliably capture:

- Crack propagation and development of the tension zone;
- Stress and strain localization within the concrete and reinforcement;
- Localization of the failure mechanism

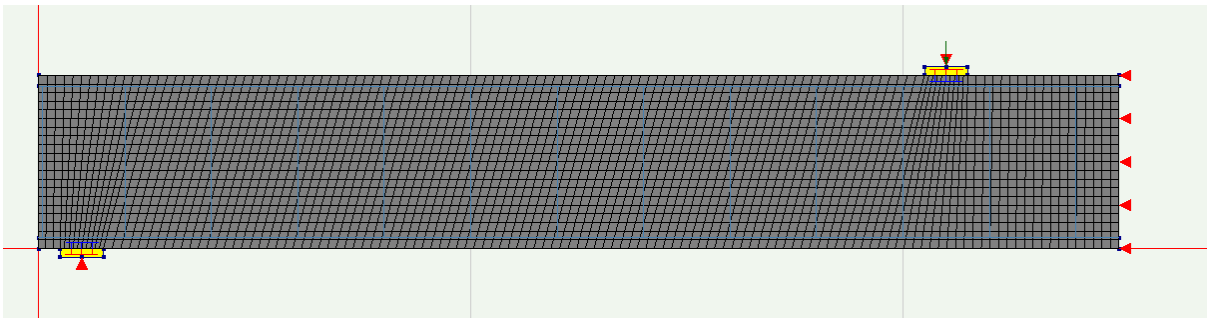

Figure 18. Finite element mesh of the RC beam, illustrating the mesh density and regular discretization for nonlinear analysis

9.2. Interpretation of Crack Development in the 2D Model

The Figures 19 a to g illustrates the progressive evolution of crack widths (E_{cw}) along a reinforced concrete beam, simulated in DIANA FEA across load range of 30 kN to 75 kN. The results depict the crack widths field extracted from the non-linear smeared crack model, providing a visual representation of damage localization and stiffness degradation.

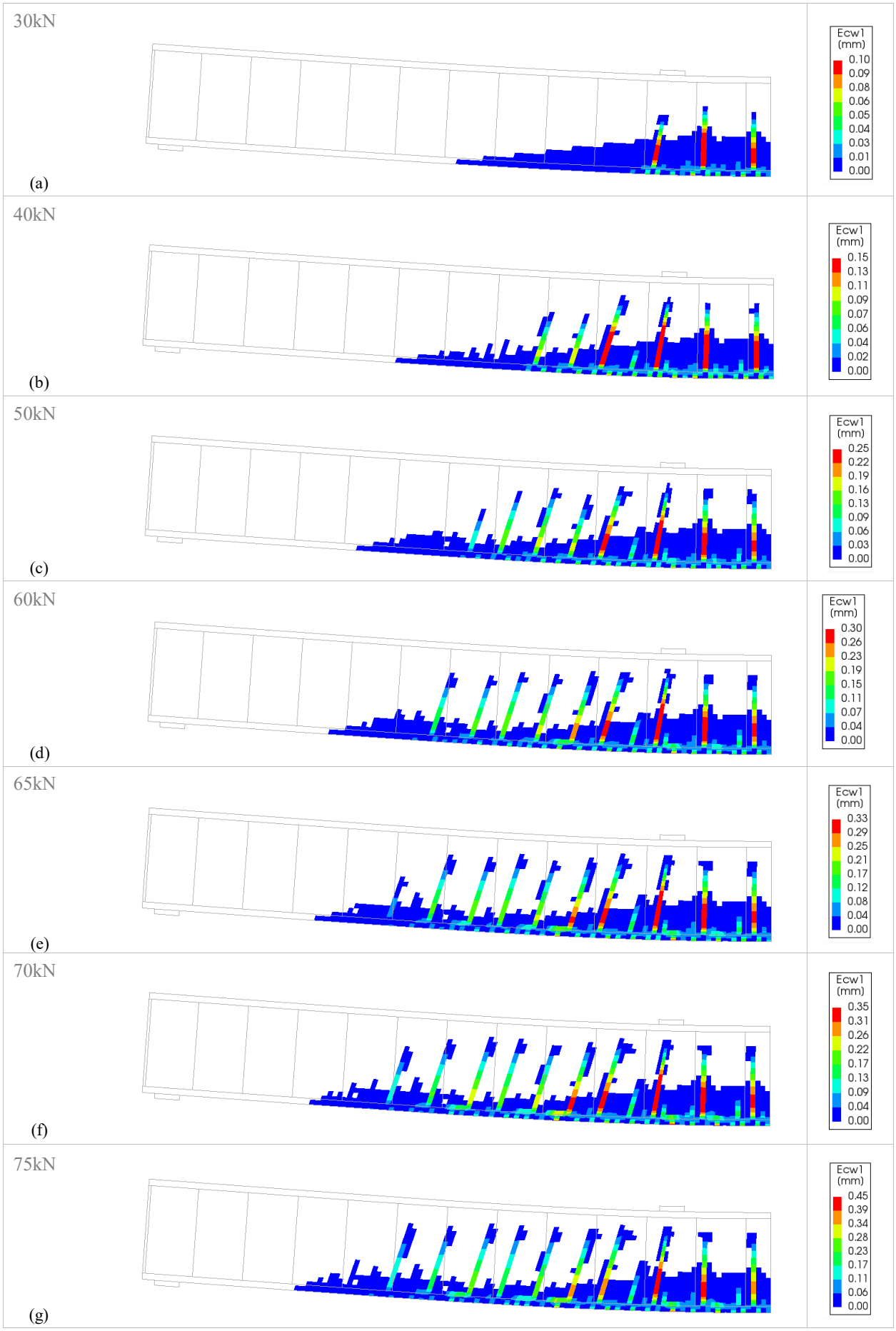

Figure 19. Development of crack widths (Ecw) in the 2D DIANA FEA model under incremental loading: a) 30 kN; b) 40 kN; c) 50 kN; d) 60 kN; e) 65 kN; f) 70 kN; g) 75 kN

In the initial loading phase (30–50 kN) shown in Figures 19 a to c, cracks are localized primarily within the extreme tension fiber where the concrete tensile strength is exceeded. During this stage, crack widths remain minimal (typically < 0.15 mm), characterizing the crack initiation phase and correlating well with the in-situ experimental observations.

As the load increases to 60–65 kN, (Figures 19 d to e), the beam transitions into a more advanced stage of crack development, characterized by the following structural behaviors:

- A significant increase in the number of cracks occurs;
- Existing cracks continue to propagate along the length and vertically toward the neutral axis;
- A gradual increase in the width of the existing cracks.

This phase marks the transition from crack initiation to a stabilized cracking state where the concrete–reinforcement interaction and the tension stiffening effect continue to contribute to the overall flexural stiffness of the beam.

At the highest load levels (70–75 kN) (Figures 19 f to g), the model exhibits the following critical response features:

- Significant crack expansion within the critical bending zones;
- Structural response is dominated by strain localization, where the most of the beam's deformation is concentrated at the primary crack interfaces;
- A rapid acceleration in crack widths is observed, signalling the onset of the failure state and the loss of serviceability.

At this stage, the E_{cw} values (crack widths) no longer represent the serviceability limit state (SLS). Instead, they serve as indicators of the activation of a nonlinear failure mechanism primarily controlled by the yielding of the reinforcement and subsequent concrete crushing

The numerical results are therefore interpreted primarily in a relative and evolutionary context, focusing on the distribution and progressive propagation of cracking under increasing load. The strong correlation between simulated crack widths at lower load levels and experimental measurements (e.g. approximately 0.15 mm at 40 kN) confirms that the smeared crack model is reasonably calibrated and suitable for characterizing the structural failure mechanism.

10. Conclusions

This study investigated the crack-width behavior of a reinforced concrete (RC) beam under four-point bending using an integrated experimental, analytical, and numerical approach. The primary objective was to evaluate the predictive accuracy of Eurocode 2, DIN 1045-1, and ACI-based formulations by benchmarking them against experimentally measured data.

The experimental investigation yields detailed observations of crack propagation, beam deflections, and reinforcement stress across incremental load levels. The results confirmed the expected correlation between width with and applied load, reflecting the characteristic behavior of RC members under flexure. While analytical calculations from various design standards reproduced this trend, there were discrepancies obvious in the predicted magnitudes.

Among the investigated methods, Eurocode 2 consistently yielded the most conservative crack-width predictions, particularly at elevated load levels. Predictions from DIN 1045-1 were slightly lower but remained aligned with those of Eurocode 2, reflecting a shared theoretical framework of the two standards. In contrast, ACI-based formulations, particularly the Gergely–Lutz model, tended to produce smaller crack-width values at higher load levels, indicating a potential tendency to underestimate crack widths compared with Eurocode-based approaches.

The comparison between analytical predictions and experimental observations highlights the critical role of accurately modeling bond behavior, crack spacing, and tension stiffening in crack-width calculations. While simplified empirical models offer practical design tools, their precision remains to reinforcement configurations and loading conditions.

As it is acknowledged that this investigation was based on a single beam specimen—limiting the statistical generality of the findings—the specimen represents a standard reinforced concrete member common in building structures. Consequently, the results establish a robust experimental benchmark for evaluating the predictive accuracy of crack-width models.

Future research should encompass a broader range of specimens featuring varied reinforcement ratios, concrete covers, and bar diameters. Additionally, expanded numerical simulations could be carried out to further refine the reliability and predictive accuracy of crack width-models used in structural design.

11. Declarations

11.1. Author Contributions

Conceptualization, V.S.H., B.S.H., A.M., and B.S.H.; methodology, V.S.H., B.S.H., A.M., and B.S.H.; software, V.S.H., B.S.H., and B.S.H.; validation, V.S.H., B.S.H., A.M., and B.S.H.; formal analysis, V.S.H., B.S.H., and A.M.; investigation, V.SH., B.S.H., A.M., and B.S.H.; resources, V.S.H. and B.S.H.; data curation, V.S.H., B.S.H., and B.S.H.; writing—original draft preparation, V.S.H. and B.S.H.; writing—review and editing, V.S.H. and B.S.H.; visualization, V.S.H. and B.S.H.; supervision, V.S.H.; project administration, V.S.H.; funding acquisition, V.S.H., B.S.H., A.M., and B.S.H.; All authors have read and agreed to the published version of the manuscript.

11.2. Data Availability Statement

The data presented in this study are available in the article

11.3. Funding

The authors received no financial support for the research, authorship, and/or publication of this article.

11.4. Conflicts of Interest

The authors declare no conflict of interest.

12. References

[1] EN 1992-1-1 (2004). Eurocode 2 – Design of Concrete Structures – Part 1-1. European Committee for Standardization (CEN) Brussels, Belgium.

[2] DIN 1045-1. (2018). Design and Construction of Concrete Structures. Deutsches Institut für Normung (DIN), Berlin, Germany.

[3] ACI 318-14. (2014). Building Code Requirements for Structural Concrete (ACI 318-14). American Concrete Institute, Michigan, United States. doi:10.14359/51688187

[4] ACI 224R-01. (2001). Control of Cracking in Concrete Structures. American Concrete Institute, American Concrete Institute, Michigan, United States. doi:10.14359/11280.

[5] Li, C. Q., & Yang, S. T. (2011). Prediction of concrete crack width under combined reinforcement corrosion and applied load. Journal of engineering mechanics, 137(11), 722-731. doi:10.1061/(ASCE)EM.1943-7889.0000289.

[6] McLeod, C. H., & Viljoen, C. (2019). Quantification of crack prediction models in reinforced concrete under flexural loading. Structural Concrete, 20(6), 2096-2108. doi:10.1002/suco.201900036.

[7] Lekshmi, U., Sherin Joseph, M., & Krishna Kumar, S. (2016). Experimental Study on Crack Width Evaluation of R.C Beams and Comparison with Various Codes. Applied Mechanics and Materials, 857, 95–100. doi:10.4028/www.scientific.net/amm.857.95.

[8] Kaklauskas, G. (2017). Crack Model for RC Members Based on Compatibility of Stress-Transfer and Mean-Strain Approaches. Journal of Structural Engineering, 143(9), 1410–1418. doi:10.1061/(asce)st.1943-541x.0001842.

[9] Sakalauskas, K., & Kaklauskas, G. (2023). Pure shear model for crack width analysis of reinforced concrete members. Scientific Reports, 13(1), 13883. doi:10.1038/s41598-023-41080-x.

[10] van der Esch, A., Wolfs, R., Fennis, S., Roosen, M., & Wijte, S. (2024). Categorization of formulas for calculation of crack width and spacing in reinforced concrete elements. Structural Concrete, 25(1), 32-48. doi:10.1002/suco.202300535.

[11] Xi, X., & Yang, S. (2017). Time to surface cracking and crack width of reinforced concrete structures under corrosion of multiple rebars. Construction and Building Materials, 155, 114-125. doi:10.1016/j.conbuildmat.2017.08.051.

[12] Sokolov, A., Valiukas, D., Praliyeva, M., Kumar, A., Bacinskas, D., & Kaklauskas, G. (2025). Experimental and Theoretical Investigation of Tension Stiffening and Curvature in Rc Beams With Extended Concrete Cover. Journal of Civil Engineering and Management, 31(2), 144–152. doi:10.3846/jcem.2025.23244.

[13] Červenka, V., Červenka, J., Rimkus, A., & Gribniak, V. (2025). Finite Element Modeling of Crack Width and Localization in Reinforced Concrete. Buildings, 15(4), 529. doi:10.3390/buildings15040529.

[14] Engström, B. (2015). Design and analysis of continuous beams and columns. Chalmers University of Technology.

[15] Shayanfar, M. A., Farnia, S. M. H., Ghanooni-Bagha, M., & Massoudi, M. S. (2020). The effect of crack width on chloride threshold reaching time in reinforced concrete members. Asian Journal of Civil Engineering, 21(4), 625–637. doi:10.1007/s42107-020-00222-6.

[16] Shang, W., Ning, X., Liu, J., & Liu, J. (2024). Failure analysis and evaluation for cracked concrete beam reinforced with CFRP. Theoretical and Applied Fracture Mechanics, 129, 104222. doi:10.1016/j.tafmec.2023.104222.

[17] Carino, N. J., & Clifton, J. R. (1995). Prediction of Cracking in Reinforced Concrete Structures. National Institute of Standards and Technology (NIST Report No. 5634), Gothenburg, Sweden.

[18] Gribniak, V., Kaklauskas, G., & Torres, L. Tension-stiffening models for serviceability analysis of reinforced concrete members. Structural Engineering and Mechanics, 90(3), 321–338. doi:10.12989/sem.2024.90.3.321.

[19] Albandar, F. A. A., Mills, G. M., & Beeby, A. W. (1975). The Prediction of Crack Widths in Reinforced Concrete Beams. Magazine of Concrete Research, 27(92), 182–184. doi:10.1680/macr.1975.27.92.182.

[20] Beeby, A. W. (2004). The influence of the parameter φ/ρ_{eff} on crack widths. Structural Concrete, 5(2), 71–83. doi:10.1680/stco.5.2.71.48276.

[21] Kattilakoski, J. (2013). Crack Control of Concrete Structures in Special Cases. Tampere University of Technology, Tampere, Finland.

[22] Yao, X., Guan, J., Zhang, L., Xi, J., & Li, L. (2021). A unified formula for calculation of crack width and spacing in reinforced concrete beams. International Journal of Concrete Structures and Materials, 15(1), 42. doi:10.1186/s40069-021-00479-4.

[23] Rusnak, C. R., Al-Hamami, A., & Menzemer, C. C. (2024). The Performance of Small Diameter Aluminum Light Support Structures Containing Handholes under Cyclic Fatigue. Open Journal of Civil Engineering, 14(2), 196–213. doi:10.4236/ojce.2024.142010.

[24] Terjesen, E., Kanstad, T., & Jensen, M. Evaluation of crack width models in reinforced concrete beams and slabs. Materials and Structures, 57, 102. doi:10.1617/s11527-024-02201-3.

[25] fib. (2013). fib Model Code for Concrete Structures 2010. International Federation for Structural Concrete (fib), Lausanne, Switzerland. doi:10.1002/9783433604090.

[26] Agarwal, H., Shariff, M. N., & Mangalathu, S. (2025). Prediction of flexural crack width of reinforced concrete beams using interpretable machine learning algorithms. Construction and Building Materials, 485, 141628. doi:10.1016/j.conbuildmat.2025.141628.

[27] Tajima, K., & Shirai, N. (2006). Numerical prediction of crack width in reinforced concrete beams by particle model. Computational Modelling of Concrete Structures, EURO-C, 221-230.

[28] Gergely, P., & Lutz, L. A. (1968). Maximum crack width in reinforced concrete flexural members. American Concrete Institute, ACI Special Publication, SP-020(2), 87–117.

[29] ACI 224.1R-07. (2007). ACI Committee 224: Causes, evaluation, and repair of cracks in concrete structures. American Concrete Institute, Michigan, United States.

[30] Hamed, T. M., & Said, A. I. (2025). Shear Strength and Serviceability of GFRP-Reinforced Concrete Beams: A Study on Varying Reinforcement Ratios. Civil Engineering Journal (Iran), 11(3), 857–883. doi:10.28991/CEJ-2025-011-03-04.

[31] BS EN 12390-2:2019. (2019). Testing hardened concrete – Part 2: Making and curing specimens for strength tests. British Standard (BSI), London, United Kingdom.

[32] BS EN 12390-3:2019. (2019). Testing hardened concrete – Part 3: Compressive strength of test specimens. British Standard (BSI), London, United Kingdom.

[33] ISO 15630-1:2019. (2019). Steel for the reinforcement and prestressing of concrete – Test methods. International Organization for Standardization (ISO), Geneva, Switzerland.